

# Appendix A

## Color Plates

The following color plates show color versions of several images in this thesis. They have been separated from the main document in order to facilitate easier printing. For ease of use, corresponding figures and color plates are cross-referenced in their captions.

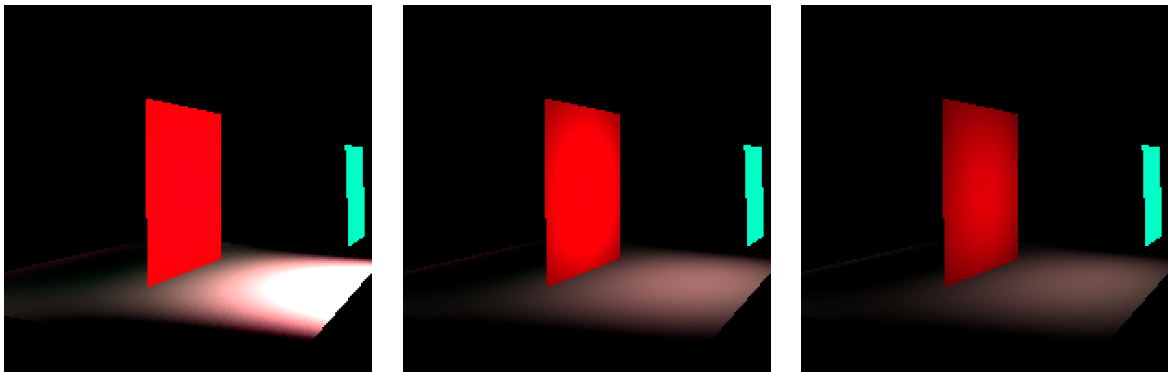


Plate A.1: A very simple example scene computed with Galerkin Radiosity but without shadow masks. The scene has been computed with basis functions of order three but different number of samples for integration (left:  $3 \times 3$ , center:  $5 \times 5$ , right:  $7 \times 7$ ). (Color version of Figure 6.15 on Page 145).

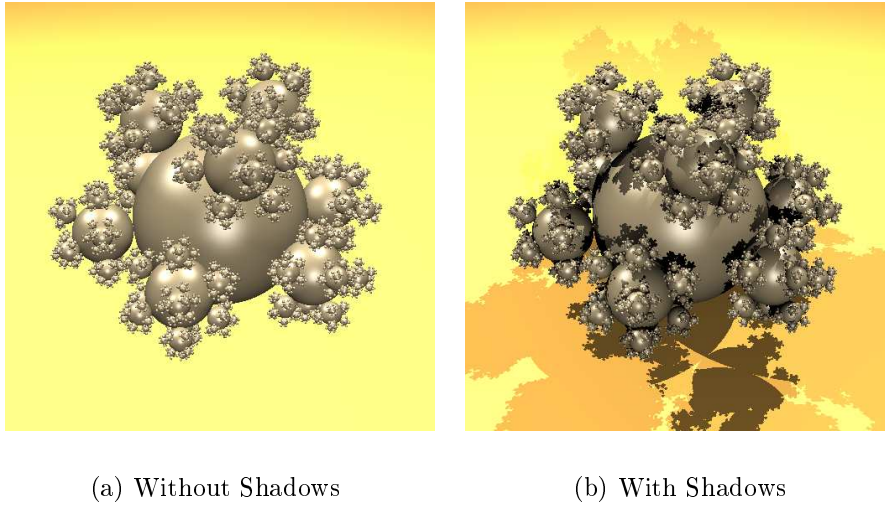


Plate A.2: The well-known “balls” scene from the SPD test package [Hai87]. The left image has been computed without shadows, the right one uses the described shadow algorithm for direct illumination. (Color version of Figure 6.6 on Page 126).

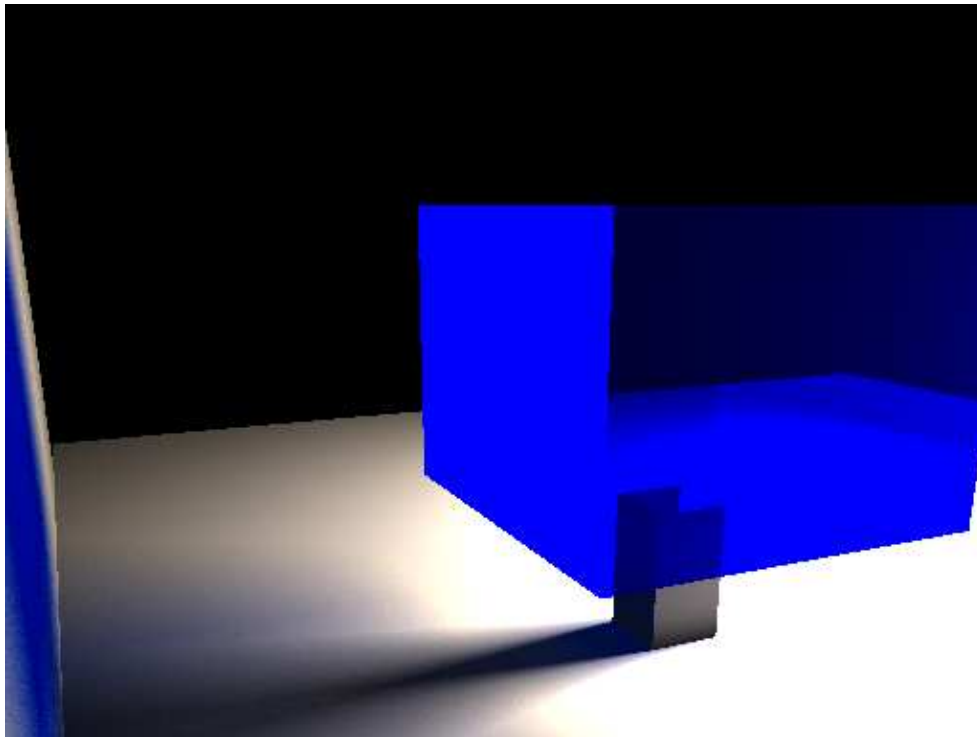


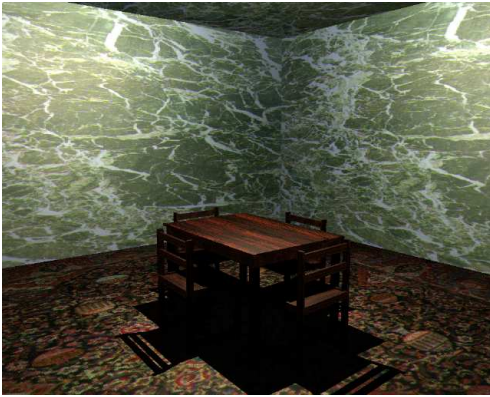
Plate A.3: A hierarchical radiosity solution applied to a scene with transparent surfaces. Note the blue shadow on the left wall and the blue color bleeding on the floor. (Color version of Figure 6.16 on Page 147).



Plate A.4: An image using Monte-Carlo path tracing to compute the global illumination. The mug on the table is reflected in a brushed metal plate. The shader describing the material of the plate uses a highly specular Phong reflection model, which is sampled appropriately by the Monte-Carlo technique. (Color version of Figure 6.8 on Page 130).



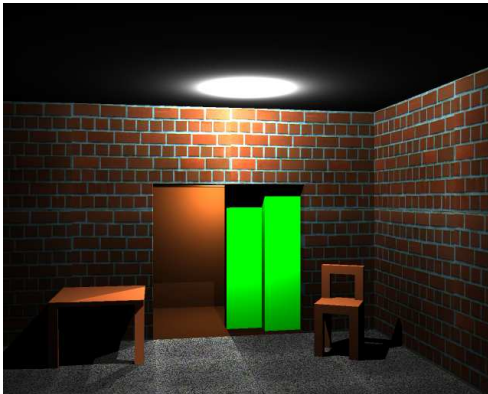
Plate A.5: A Wavelet Radiosity solution using shadow masks to better approximate high shadow gradients. Third-order Multiwavelets are used as basis functions. Note the sharp shadow from the lamp on the desk and the floor. (Color version of Figure 6.21 on Page 152).



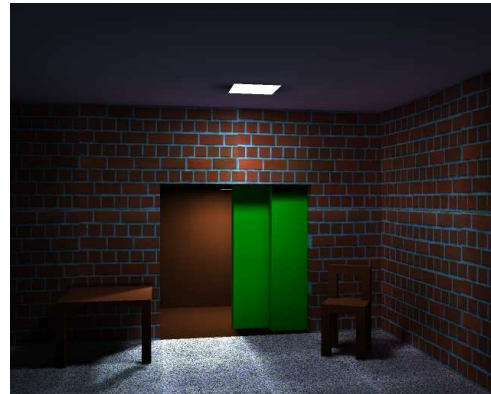
(a) Ray tracing



(b) Wavelet Radiosity



(c) Ray Tracing



(d) Wavelet Radiosity

Plate A.6: Two approximations of global illumination in a scene with textured surfaces: on the left using direct illumination with a point light approximation and ray traced shadows, and on the right with a quadratic wavelet radiosity solution. (Color version of Figure 6.24 on Page 158).

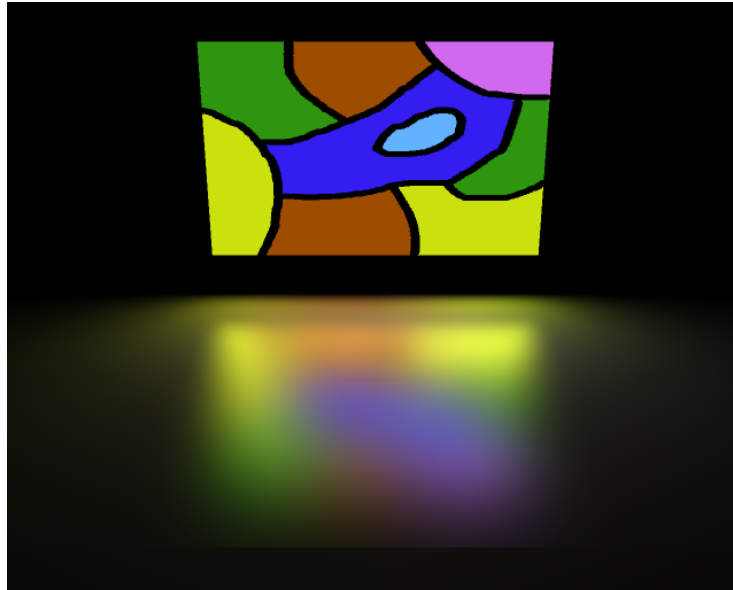


Plate A.7: A simple image computed with Wavelet Radiance demonstrating the effects of the directionally dependent computation. The floor has a Phong-like reflection behavior, showing a diffuse reflection near the window and a specular reflection that gets blurrier near the viewer. (Color version of Figure 6.22 on Page 154).



Plate A.8: An image showing the integrated rendering of surface and volume data in the Vision architecture. This image was rendered with direct illumination and a ray tracing renderer. The volume object above the desk is projected onto the wall and the desk as well as viewed directly. (Color version of Figure 6.25 on Page 162).



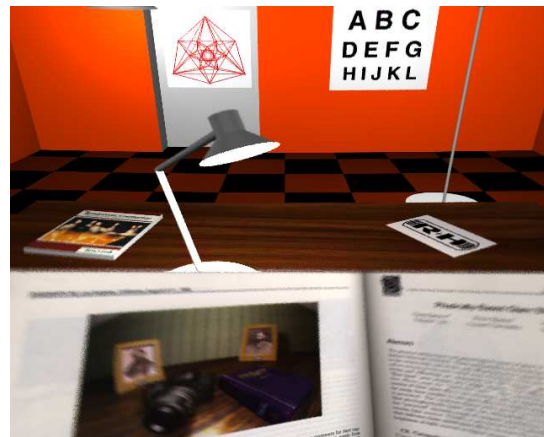
(a) Uncorrected



(b) Near focus



(c) Far focus



(d) PAL lens

Plate A.9: Simulation of a human eye that lost the ability to adjust focus with a fixed accommodation to 1 meter (a). The same eye corrected with a lens for reading (b), driving (c), and with a “progressive addition lens” (d). All images have been computed with Vision using a special Lenses and Camera subsystem for simulating the behavior of the human eye and the optical properties of the lenses. Wavefront tracing and distribution tracing has been used for computing the optical properties of the lens and the depth-of-field, respectively [LGS<sup>+</sup>95]. (Color version of Figure 6.27 on Page 166).





Plate A.10: An example image of a bathroom computed with ray tracing. Also see color Plate 7.1. (Color version of Figure 7.1 on Page 174).

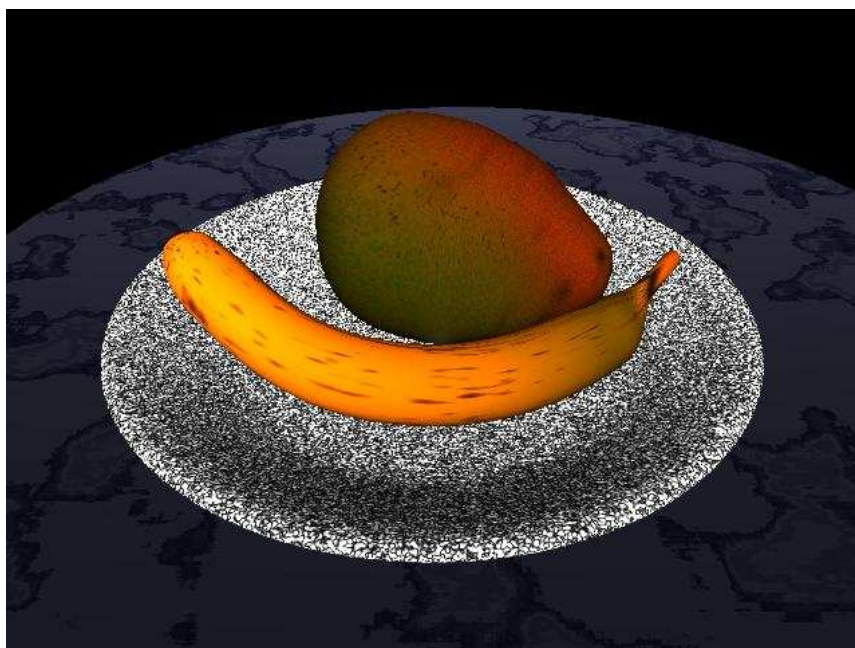
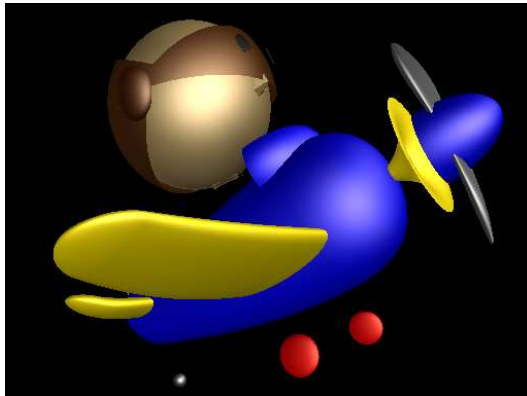


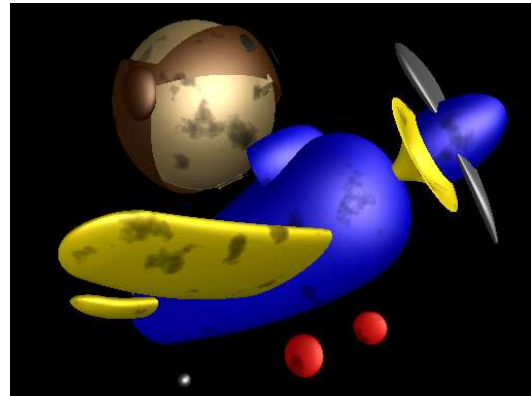
Plate A.11: An example image showing two special surface shaders “mango” and “banana”. Additionally, “granite” and “marble” shaders have been used. (Color version of Figure 8.1 on Page 193).



Plate A.12: Three recursive shaders applied to the floor. The checker board shader calls two different marble shaders and performs bump mapping at the edges of the tiles. (Color version of Figure 8.2 on Page 205).



(a) Plain



(b) With layered "dirt" shader

Plate A.13: The use of layered shaders. On the left, plastic shaders are applied to the model. On the right, a "dirt" shader is layered onto the unmodified plastic shaders. (Color version of Figure 8.3 on Page 206).



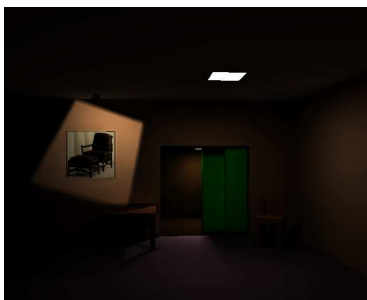


(a) Min-max operator



(b) Ward's operator

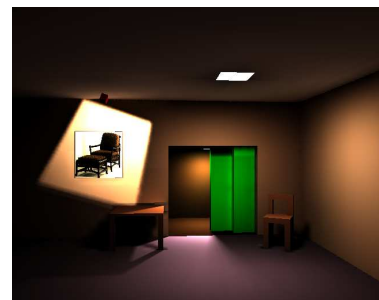
Plate A.14: Comparing a min-max-scaling operator to Ward's tone-mapping operator [War94] both applied to the same dark scene. Note that Ward's operator maintains the impression of darkness in the scene. (Color version of Figure 9.5 on Page 220).



(a) Low



(b) Medium



(c) High

Plate A.15: The tone reproduction operator from Tumblin and Rushmeier [TR93] for the same scene with a low, medium, and high illumination. (Color version of Figure 9.8 on Page 222).

